Structural and Voltammetric Studies on the Reduction of the Bis(2,2′-bipyridyl)platinum(II) Cation in Aprotic Media

Alan R. Brown,*,† Zijian Guo,† Fred W. J. Mosselmans,‡ Simon Parsons,† Martin Schröder,§ and Lesley J. Yellowlees*,†

Contribution from the Department of Chemistry, University of Edinburgh, West Mains Road, Edinburgh EH9 3JJ, U.K., Synchrotron Radiation Department, Daresbury Laboratory, Daresbury, Cheshire WA4 4AD, U.K., and Department of Chemistry, University of Nottingham, Nottingham NG7 2RD, U.K.

Received May 14, 1998

Abstract: The reduction of the bis(2,2′-bipyridyl)platinum(II) cation, $[Pt(bpy)_2]^{2+}$, in aprotic media has been studied electrochemically. Voltammetry at scan rates above 500 V s^{-1} reveals three reversible reductions at −1.14, −1.45, and −2.07 V versus the ferrocenium/ferrocene couple. The first of these couples shows only a moderately fast electron transfer. At lower scan rate, e.g., 0.1 V s^{-1}, or on the time scale of an electrosynthesis, the product of the first one-electron reduction is shown to be the previously unknown homoleptic platinum(I) dimeric cation (μ_2-2,2′-bipyridyl)bis(2,2′-bipyridyl)bisplatinum(I), $[Pt_2(bpy)_3]^{2+}$, an X-ray crystal structure of which is presented along with 2-D NMR and EXAFS results showing this is also the major species in solution. The formation of $[Pt_2(bpy)_3]^{2+}$ is shown by digital simulation of voltammetric results to be by a first-order process initiated by one-electron reduction of $[Pt(bpy)_2]^{2+}$, and subsequent ligand loss before insertion into the Pt−N bond of another molecule of reduced monomer. Electrolysis in the absence of inert electrolyte is shown to be a viable means of producing pure samples of the products of electrode reactions, even in cases where these are delicate or unstable.

Introduction

The chemistry and electrochemistry of homoleptic transition metal complexes with 2,2′-bipyridyl (bpy) are well-known and have been thoroughly reviewed.[1] While many of these species exhibit a range of easily accessible reversible couples in aprotic organic media, some show redox-induced reactions including bpy loss and increased electrophilicity, examples being the reduction of $[Rh(bpy)_3]^{2+}$ to yield[2] $[Rh(bpy)_2]^{+}$, and the highly reactive species $[Cu(bpy)_2]^{+}$, generated in the reduction of $[Cu(bpy)_3]^{2+}$, which coordinates dioxygen reversibly and is a catalyst in the oxidation of alcohols.[3,4] The behavior of $[Pt(bpy)_2]^{2+}$ is at least as complex as in these two cases, and to date unresolved. The first reduction of this cation in such solvents as *N*,*N*-dimethylformamide and methyl sulfoxide has been shown previously to be irreversible, and followed by two reversible reductions of the product of the first reduction.[5,6] The reduction of the complex by metallic iron or at a platinum or indium tin oxide electrode in water has recently been shown[7] to give the complex $[Pt(bpy)_2]^{+}$ which crystallizes spontaneously to give a black, filamentous, electrically conducting material, which shows weak bonding interactions between the stacked platinum(I) centers. Given the stability of this complex, we wish to understand the electrochemical response of $[Pt(bpy)_2]^{2+}$ in aprotic solvents, and particularly to establish the product of the reaction following the first electron transfer as revealed voltammetrically.[5,6]

The structural characterization of a transition metal complex depends primarily on nuclear magnetic resonance spectroscopy, mass spectroscopy, and X-ray crystallography. We were faced with the problem of obtaining a pure sample of a compound which had only been produced voltammetrically. Classical chemical reductants were likely to pose problems related to the proximity of the couples following the first reduction of $[Pt(bpy)_2]^{2+}$ and the "noninnocent" nature of many of the one-electron reductants.[8] Bulk electrolysis serves the purpose well, the redox potential being tuneable, essential in such an electrochemically rich system. However, there remains the problem of isolating the target complex from the supporting electrolyte, although this has been achieved in the past for certain systems.[9] We decided instead to use the complex itself, as the tetrafluoroborate salt, as its own supporting electrolyte in a fritted bulk electrolysis cell designed to be of the smallest possible volume, to keep the concentration of the analyte at a maximum. The solution, once subjected to electrolysis, could then be characterized by ^{1}H NMR spectroscopy, if carried out in a deuterated solvent, without interference from the alkyl protons of the tetraalkylammonium salts usually employed as supporting electrolyte, or worked up to yield a pure solid. Extended X-ray

† University of Edinburgh.
‡ Daresbury Laboratory.
§ University of Nottingham.

(1) Constable, E. C. *Adv. Inorg Chem.* **1989**, *34*, 1−63.
(2) Kew, G.; De Armond, K.; Hanck, K. *J. Phys. Chem.* **1974**, 727−734.
(3) Munakata, M.; Nishibayashi, S.; Sakamoto, H. *J. Chem. Soc., Chem. Commun.* **1980**, 219−220.
(4) Pecht, I.; Anbar, M. *J. Chem Soc. A* **1968**, 1902.
(5) Chassot, L.; von Zelewsky, A. *Inorg. Chem.* **1987**, *26*, 2814−2818.
(6) Braterman, P. S.; Song, J.-I.; Wimmer, F. M.; Wimmer, S. *Inorg. Chim. Acta* **1991**, *189*, 7.
(7) Palmans, R.; MacQueen, D. B.; Pierpoint, C. G.; Frank, A. J. *J. Am. Chem. Soc.* **1996**, *118*, 12647−12653.
(8) Connelly, N. G.; Geiger, W. E. *Chem. Rev.* **1996**, *96(2)*, 877−910.
(9) See for example: (a) Yamamoto, Y.; Takahashi, K.; Yamazaki, H. *J. Am. Chem. Soc.* **1986**, *108* (9), 2458−2459. (b) Tanase, T.; Kawahara, K.; Ukaji, H.; Kobayashi, K.; Yamazaki, H,; Yamamoto, Y. *Inorg. Chem.* **1993**, *32*, 3682−3688.

S0002-7863(98)01670-9 CCC: $15.00
Published on Web 08/18/1998

absorption fine structure spectroscopy (EXAFS) measurements remain possible, as they are in the presence of supporting electrolyte. Voltammetry is also feasible[10] at normal electrodes and scan rates, allowing one to be certain that the product of the electrolysis is the one desired.

Experimental Section

Materials. $[Pt(bpy)_2][BF_4]_2$ was synthesized by reaction of K_2PtCl_4 (0.5 g, 1.2 mmol, Johnson Matthey) and 2,2′-bipyridyl (1.38 g, 8.9 mmol, Aldrich) in deionized water (65 mL) and heating until complete dissolution of the initially formed $[Pt(bpy)Cl_2]$ had occurred. The hot solution was filtered, $NaBF_4$ (0.52 g, 4.8 mmol, Hopkin and Williams) added, and the whole refrigerated overnight. The canary yellow crystalline product was isolated and recrystallized from the minimum quantity of boiling deionized water, yield 0.60 g, 73%, and gave satisfactory elemental analysis (C, H, N). $[N^nBu_4][BF_4]$, prepared by the neutralization of tetrabutylammonium hydroxide with tetrafluoroboric acid (both Fluka), was recrystallized twice from a 1:1 water/methanol mixture and dried at 343 K *in vacuo* for 48 h.

The air-sensitive orange compound $[Pt_2(bpy)_3][BF_4]_2$ was synthesized by potentiostatic electrolysis (−1.3 V versus $FeCp_2^{+/0}$) at a platinum gauze working electrode in a two-compartment, all glass, fritted, gastight cell of reduced dimensions, the design of which is contained in the Supporting Information. The working electrode compartment was of volume 2 cm^3 and contained $[Pt(bpy)_2][BF_4]_2$ at a concentration of 0.05 mol dm^{-3} in either *N*,*N*-dimethylformamide (Aldrich, anhydrous 99.8%) or methyl sulfoxide-d_6 (Aldrich, 99.9 atom % D). Conversion rates were typically in the 10 μmol h^{-1} range, i.e., a current of around 0.3 mA. The reference electrode, a silver wire (Goodfellow, 99.999%) electrolytically coated with silver chloride, was contained in a Luggin capillary and directly immersed in the contents of the working electrode compartment. This unconventional arrangement gave stable potential measurements and, due to the small internal diameter of the tip of the capillary, effectively isolated the electrolyzed solution from the surface of the silver wire. The counter electrode, also of platinum gauze, was separated by a grade 3 fritted disk from the working electrode compartment, and was immersed in a solution of $[N^nBu_4][BF_4]$, 0.05 mol dm^{-3}, in the solvent present in the working electrode compartment. The progress of electrolysis was monitored by coulometry and by cyclic voltammetry at a 500 μm diameter platinum disk electrode. After electrolysis, a cyclic voltammogram was recorded and the product removed from the cell through a cannula under pressure of argon. Crystals suitable for X-ray analysis were produced by layering the reaction liquor resulting from the reduction in *N*,*N*-dimethylformamide with argon-saturated, sodium-dried diethyl ether (Rectapur, Prolabo) in a Schlenk tube of internal diameter 7 mm. Diffusion of these two solvents at room temperature produced orange blocklike crystals. The sample for NMR spectroscopy resulted from the reduction in methyl sulfoxide-d_6, and was transferred directly into an argon-filled NMR tube equipped with a vacuum tap and rubber septum. The tube was capped and sealed with high-vacuum wax in an argon-filled drum.

Electrochemistry. Electrochemical experiments were performed using a DELL 466 DL personal computer running GPES 4.4 software (Eco Chemie) to drive an Autolab PGSTAT20 potentiostat, the ohmic drop compensation facility of which was used in all voltammetric experiments. An Ag/AgCl/$[N^nBu_4]$Cl, 0.05 mol dm^{-3}, $[N^nBu_4][BF_4]$, 0.45 mol dm^{-3}/dichloromethane reference electrode was employed for voltammetry, but all potentials are quoted relative to the ferrocenium/ferrocene ($Cp_2Fe^{+/0}$) couple. Voltammetric measurements were carried out in a conventional three-electrode cell, the working electrode being a platinum microdisk of nominal diameter 500 or 25 μm as appropriate, which was routinely polished using a 3000 Å alumina slurry (Presi). Solutions were purged with a stream of solvent-saturated argon (BOC Gases). The cell was thermostated at 293.2 ± 0.1 K for all voltammetric experiments by means of a Haake Q cooling bath fitted with an F-3 temperature controller. Electrosynthetic experiments were carried out at ambient temperature. Simulations of voltammetric experiments were carried out using a DCS personal computer equipped with a Pentium-S CPU running Antigona32 software written by Dr. Loïc Mottier of the Università di Padova, available at http://www.chemistry.unipd.it.

EXAFS Measurements. The Pt L3-edge X-ray absorption spectra were obtained on Station 9.2 at the SRS, CCLRC Daresbury Laboratory. The ring current was around 180 mA in the 2 GeV storage ring. The monochromator was calibrated using a Pt foil with the Pt L3-edge at 11 554 eV. Data were collected using a Si(220) double-crystal monochromator, detuned to 50% of the maximum intensity to remove higher harmonics. The sample was in the form of a frozen solution 5 mmol dm^{-3} in the complex of interest in a 0.2 mol dm^{-3} $[N^nBu_4][BF_4]$/*N*,*N*-dimethylformamide solution, held in poly(methyl methacrylate) cells with Kapton windows. A liquid nitrogen cryostat was employed to maintain the cell at 80 K during data collection. Data were recorded to $k = 13.5$ $Å^{-1}$ in fluorescence mode using a Canberra 13-element solid-state Ge detector, and three data sets were averaged to improve the data quality.

The data were calibrated in the SRS program EXCALIB and background subtracted using the SRS program EXBROOK. EXAFS data analyses were also performed using EXCURV92.[11] Phase shifts were calculated *ab initio* using Hedin−Lundqvist exchange potentials and von Barth ground-state potentials. Coordination numbers were not refined. Shells were checked for their significance using the Joyner test.[12] The fit index *R* that is quoted in Table 4 is defined by

$$R = \sum_{(i)}[(1/(\sigma_{(i)})|\text{experiment}_{(i)} - \text{theory}_{(i)}|)] \times 100$$

where

$$1/(\sigma_{(i)}) = ([k_{(i)}]^3/\sum_{(i)}[k_{(i)}]^3|\text{experiment}_{(i)}|)$$

X-ray Crystallography. Crystals of $[Pt_2(bpy)_3][BF_4]_2$ were picked at low temperature from under RS3000 perfluoropolyether oil and data collected on a Stoe Stadi-4 diffractometer equipped with an Oxford Cryosystems low-temperature system operating at 150 K. Data were collected using Cu Kα radiation and on-line profile fitting,[13] with the aim of maximizing I/σ for measured intensities. An absorption correction based on ψ-scans was applied. The structure was solved by direct methods (Shelxs-96)[14] and refined against *F* by full-matrix least squares using data with $F > 4\sigma(F)$ (CRYSTALS).[15] Crystal data and details of the refinement are given in Table 1.

NMR Spectroscopy. NMR spectra were recorded using a Varian Inova 600 MHz spectrometer, the ^1H chemical shifts being internally referenced to sodium 3-(trimethylsilyl)-1-propanesulfonate (TSP) at 0 ppm. Gradient-selected H,H-COSY experiments were carried out using the standard pulse sequence. Data sets with 2048 × 512 points were acquired with sweep widths of 4000 Hz in both dimensions and 16 scans per t_1 increment. The t_1 dimension was zero-filled to 2048 data points, and the spectrum was processed with a combination of exponential and Gaussian weighting functions.

Results and Discussion

Figures 1 and 2 show cyclic voltammograms for a 10.23 mmol dm^{-3} solution of $[Pt(bpy)_2][BF_4]_2$ at 0.1 and 500 V s^{-1}, respectively. No waves attributable to the platinum complex could be detected within the positive range of this solvent, or methyl sulfoxide or propylene carbonate, which gave otherwise similar results. Voltammetry of a stirred solution allowed all waves shown to be assigned as reductions. The first wave in

(10) Typical voltammograms for the $[Pt(bpy)_2]^{2+}$ system without inert electrolyte before and after electrolysis, necessarily distorted by ohmic drop, are presented in the Supporting Information.

(11) Binsted, N.; Campbell, J. W.; Gurman, S. J.; Stephenson, P. C. SERC Daresbury Laboratory EXCURV92 program, 1991.
(12) Joyner, R. W.; Martin, K. J.; Meehan, P. *J. Phys. C* **1987**, *20*, 4005−4012.
(13) Clegg, W. *Acta Crystallogr.* **1981**, *A37*, 22−28.
(14) Sheldrick, G. M. Shelxs-96, Program for the solution of crystal structures, University of Göttingen, Germany, 1996.
(15) Watkin, D. J.; Prout, J. R.; Carruthers, J. R.; Betteridge, P. W. CRYSTALS Issue 10, Chemical Crystallography Laboratory, University of Oxford, 1996.

Table 1. Crystal Data, Data Collection Conditions, and Solution Refinement Details for $[Pt_2(bpy)_3][BF_4]_2$

empirical formula	$C_{30}H_{24}N_6B_2F_8Pt_2$
formula weight	1032.34
wavelength	1.541 80 Å
temperature	150 K
crystal system	monoclinic
space group	*C*2/*c*
unit cell dimensions	$a = 15.387(8)$ Å, $\alpha = 90°$ $b = 10.878(5)$ Å, $\beta = 101.22(5)°$ $c = 18.142(9)$ Å, $\gamma = 90°$
volume	2978.36 Å^3
number of reflections for cell	67 ($20° < \theta < 22°$)
Z	4.00 (2-fold axis bisects Pt−Pt bond)
density (calculated)	2.30 Mg m^{-3}
absorption coefficient	18.27 mm^{-1}
F(000)	1899.43
crystal description	orange block
crystal size	0.31 × 0.25 × 0.24 mm
θ range for data collection	10−140°
index ranges	$-18 \le h \le 18$, $-9 \le k \le 13$, $-9 \le l \le 22$
number of reflections collected	2789
number of independent reflections	2624 [$R_{(int)} = 0.02$]
scan type	$\omega-\theta$ with learnt profile
absorption correction	ψ-scans ($T_{min} = 0.018$, $T_{max} = 0.120$)
hydrogen atom placement	geometric
hydrogen atom treatment	placed geometrically after each cycle
data/number of parameters	2421/218
goodness of fit	1.0832
R^a	0.0387
$R_W{}^b$	0.0474
observed criterion	$>2.00\sigma(I)$
extinction coefficient	1.1(6)
final maximum Δ/σ	0.007
weighting scheme	Chebychev three-term polynomial
largest diffraction peak and hole	1.51 and −1.47 e Å^{-3}

[a] $R = \sum|F_o - F_c|/\sum F_o$. [b] $R_w = \sum w(F_o - F_c)^2/\sum wF_o^2$.

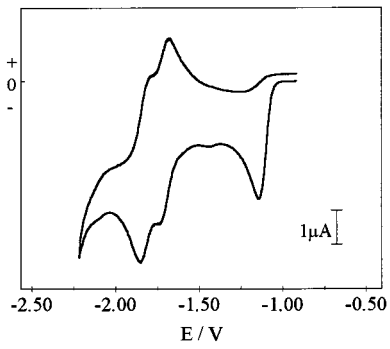

Figure 1. Voltammogram of $[Pt(bpy)_2][BF_4]_2$ (10.23 mmol dm^{-3}) in *N*,*N*-dimethylformamide/0.2 mol dm^{-3} [N^nBu_4][BF_4] recorded at a 500 μm diameter electrode with scan rate 0.1 V s^{-1}.

Figure 1, with forward peak potential −1.1 V, was found by bulk electrolysis to correspond to the consumption of 1.1 ± 0.1 electrons per molecule of starting material. Table 2 summarizes these voltammetric data; the electron stoichiometries for waves **2** and **5** (see Figure 2) are by comparison with wave **1** at high scan rate. Waves **3** and **4** (see Figure 1) are too close to resolve by bulk electrolysis, but a reduction at −2.1 V showed the total charge passed to correspond to 1 electron within experimental error. Simulation confirmed that these nearly superimposed waves are of equal height. Exhaustive electrolysis at −1.3 V yielded an orange solution, a cyclic voltammogram of which showed only waves **3** and **4** at their original height, and no trace of waves **1**, **2**, and **5** as seen in Figure 1. Taking

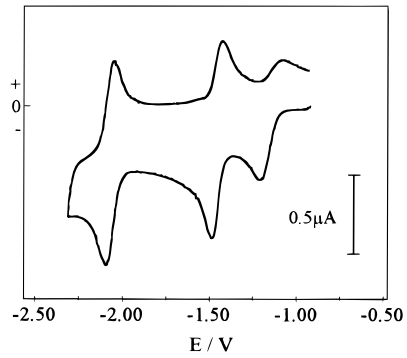

Figure 2. Voltammogram of $[Pt(bpy)_2][BF_4]_2$ (10.23 mmol dm^{-3}) in *N*,*N*-dimethylformamide/0.2 mol dm^{-3} [N^nBu_4][BF_4] recorded at a 25 μm diameter electrode with scan rate 500 V s^{-1}.

Table 2. Summary of Voltammetric Data for $[Pt(bpy)_2][BF_4]_2$ in *N*,*N*-Dimethylformamide/0.2 mol dm^{-3} [N^nBu_4][BF_4]

wave	$E_{1/2}$ (V)	no. of electrons	wave	$E_{1/2}$ (V)	no. of electrons
1	−1.14[a]	1	**4**	−1.81	0.5
2	−1.45[a]	1	**5**	−2.07[a]	1
3	−1.71	0.5			

[a] Data obtained from voltammogram run at 500 V s^{-1}.

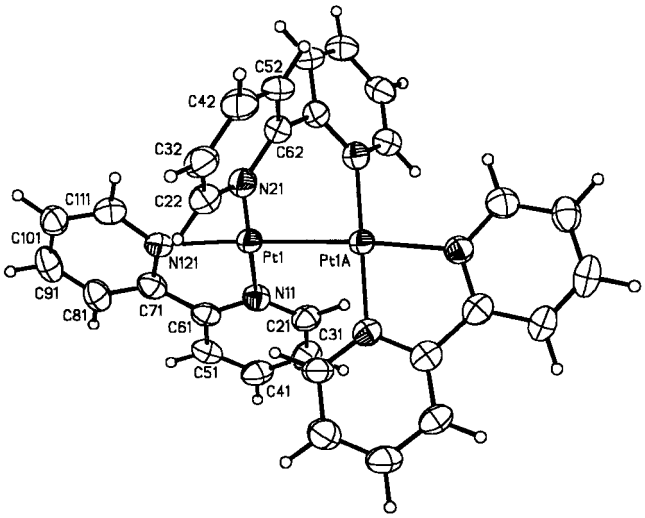

Figure 3. Thermal ellipsoid (50% probability) plot for the complex $[Pt_2(bpy)_3]^{2+}$ (with numbering scheme).

these data into account, it seemed likely that the voltammetric response shown in Figure 2 is due to a series of monomeric complexes $[Pt(bpy)_2]^{2+/+/0/1-}$, of which all but the first are unstable at room temperature. The irreversibility of wave **1** at moderate scan rates is plainly a result of a reasonably fast following reaction, and at scan rates of around 20 V s^{-1} waves **1**−**5** are present in approximately equal intensity.

The orange solution obtained after passage of one molar equivalent of electrons at −1.3 V was found to be EPR silent. Taken together with the electron stoichiometry of waves **3** and **4** which are due to the redox chemistry of the product of the reaction initiated by the first electron transfer, this led us to the conclusion that the product is a Pt(I)−Pt(I) dimer. Waves **3** and **4** then correspond to the transfer of one electron *per molecule of dimer*.

The structure of $[Pt_2(bpy)_3]^{2+}$ is shown in Figure 3. Selected bond distances (Å) and angles (deg) are given in Table 3. The complex cation consists of two platinum centers joined by a Pt−Pt σ-bond supported by a 2,2′-bipyridine ligand bridging the two metal centers. The Pt−Pt distance of 2.5272(5) Å is

Table 3. Selected Bond Lengths and Angles for $[Pt_2(bpy)_3][BF_4]_2$

bond	length (Å)	fragment	angle (deg)
Pt1−Pt1A	2.5272(5)	N21−Pt1−Pt1A	81.7(1)
Pt1−N21	2.020(5)	Pt1A-Pt1−N11	97.3(1)
Pt1−N121	2.132(7)	N11−Pt1−N121	78.9(2)
Pt1−N11	2.019(5)	N121−Pt1−N21	102.1(2)
N21−C22	1.343(7)	N21−Pt1−N11	177.2(2)
N21−C62	1.353(7)	N121−Pt1−Pt1A	176.1(1)
N121−C111	1.360(8)	Pt1−N21−C62	121.8(4)
N121−C71	1.350(8)	Pt1−N11−C61	116.5(4)
N11−C21	1.328(7)	Pt1−N121−C71	113.2(4)
N11−C61	1.370(7)	Pt1−N21−C62	121.8(4)
C62−C62A	1.49(1)	Pt1−N11−C21	124.7(4)
C61−C71	1.476(8)	Pt1−N121−C111	126.9(4)

consistent with a bridged single bond between two Pt(I) centers.[16] Each metal atom is located in a square-planar arrangement formed by two N atoms from a bidentate 2,2′-bipyridine ligand, one N atom from the bridging 2,2′-bpy ligand and the second Pt atom. The dihedral angle formed by the best least-squares planes defined by each platinum environment is 67.1°.

The bridging 2,2′-bipyridine ligand is nonplanar with the two pyridine rings rotated about the C(62)−C(62A) bond, the torsion angle N(21)−C(62)-C(62A)−N(21A) being 55.3(7)°. The bridging C−C bond length of 1.49(1) Å is the same as the equivalent distance in the bidentate bpy ligands. This is a remarkable coordination mode for 2,2′-bipyridine which usually binds in a chelating manner. There are only a few platinum(II) and paladium(II) complexes containing a bridging 2,2′-bipyridine ligand,[17] and it should be noted that we could find no other examples in the literature of complexes containing a 2,2′-bipyridine ligand bridging a metal−metal bond.

There is no significant lengthening of the Pt−N bonds between those found in Pt(II)−bpy complexes such as $[Pt(bpy)Cl_2]$[18] and $[Pt(bpy)_2][NO_3]_2$[19] and the dimer described here. A similar observation was also noted[7] for the linear chain complex $[Pt(bpy)_2]^+$. This observation suggests that upon reduction the additional electron does not enter a primarily $d_{x^2-y^2}$ orbital on the Pt, but rather an orbital which is perpendicular to the PtN_3 plane, presumably the $6p_z$-based Pt orbital. This is consistent with our earlier interpretation of the EPR spectra of monoreduced $[Pt(bpy)X_2]^-$ complexes based on a semi-occupied molecular orbital including a significant amount of Pt $6p_z$ character.[20]

Voltammetry of a sample of $[Pt_2(bpy)_3][BF_4]_2$ in *N*,*N*-dimethylformamide/$[N^nBu_4][BF_4]$, 0.2 mol dm^{-3}, revealed a response identical to that of the product of the one-electron reduction of $[Pt(bpy)_2][BF_4]_2$. To confirm that this crystalline sample and the species in solution were identical, we undertook an EXAFS study to determine the metal coordination environment, and an ^1H NMR study to determine the ligand arrangement. Table 4 shows the results for the coordination environment of each platinum atom from the EXAFS analysis of the orange solution. The nitrogen shell could not be resolved into two shells and is dominated by the nearer atoms, and the large static disorder in this shell leads to a shortening in the distance obtained by EXAFS analysis as the harmonic assumption inherent in the EXCURV92 treatment used here breaks down.[21] Graphic evidence of the fit between theory and experiment is given in the Supporting Information. Data presented in Table 4 confirm that the product of wave **1** is dimeric and consistent with the single-crystal X-ray structure presented.

Table 4. EXAFS Results for the Coordination Shell of Each Platinum Atom in the Complex Produced by the One-Electron Reduction of $[Pt(bpy)_2][BF_4]_2$ in *N*,*N*-Dimethylformamide[a]

neighboring atom(s)	EXAFS distance (Å) (±1%)	mean crystallographic distance (Å)	Debye−Waller factor ($Å^{-2}$)	fit index
Pt	2.55	2.527	0.016	46.6
3N	2.01	2.057	0.006	
6C	2.95	2.974	0.018	

[a] Single-crystal data for $[Pt_2(bpy)_3][BF_4]_2$ are included for comparison.

Figure 4 shows the ^1H NMR spectrum of the orange reaction liquor obtained after electrolysis in methyl sulfoxide-d_6, and a 2-D COSY spectrum for the same sample. The NMR data are summarized in Table 5, excluding the instrumental "wrapover" peak at 10 ppm in the COSY spectrum. The twelve cross-peaks present in the COSY spectrum show the sixteen signals to be related in four groups of four: (1, 5, 9, and 15), (2, 8, 10, and 14), (3, 7, 12, and 16), and (4, 6, 11, and 13). Furthermore, the pattern of coupling is consistent with the spectrum corresponding to four different pyridyl environments. The group (3, 7, 12, and 16) was assigned to free 2,2′-bipyridyl by comparison with the spectrum of an authentic sample recorded under the same conditions. The remaining three types of pyridyl environments observed are consistent with the structure of $[Pt_2(bpy)_3]^{2+}$ and, together with the EXAFS results, confirm that the binuclear Pt(I)−Pt(I) species is the electroactive component of the orange solution which is characterized by waves **3** and **4** (see Figure 1).

In addition, the NMR spectrum can now be fully assigned, as detailed in Table 5, the atom numbering scheme being as for Figure 3. The group (2, 8, 10, and 14) is assigned to the protons on the bridging bpy ligand given the shift to lower frequency of the resonance for the 3-position in this group, H52, than that of the proton in the 4-position in the same ring, H42. This unusual situation is consistent with a ligand twisted about the 2,2′-bond, as the effect of the aromatic ring currents in the second ring on the proton in the 4-position is lessened. The resonance for H81 at 8.05 ppm is very low for a proton on the 6-position of a bipyridyl ring, but may be assigned as such since it couples to only one other proton, and due to the splitting of 5.2 Hz observed, consistent only with this assignment.[22] The low value of the chemical shift is almost certainly due to the ring currents in the symmetry-related ring attached to the second platinum atom, which is 3.9 Å away, facing this proton, as shown in Figure 3. The final group of four resonances are then due to H81, 91, 101, and 111.

(16) (a) Uson, R.; Fornies, J.; Espinet P.; Fortuno, C.; Milagros, T.; Welch, A. J. *J. Chem. Soc., Dalton. Trans.* **1989** 1583−1587. (b) Betz, P.; Bino, A. *J. Am. Chem. Soc.* **1988**, *110* 602−603 and references therein.

(17) (a) Uson, R.; Fornies, J.; Thomas, M.; Casas, J. M.; Fortuno, C. *Polyhedron* **1989**, *8*, 2209−2211. (b) Fornies, J.; Navarro, R.; Sicilia, V.; Tomas, M. *Inorg. Chem.* **1993**, *32*, 3675−3681.(c) Uson, R.; Fornies, J.; Tomas, M.; Martinez F.; Casas, J. M.; Fortuno, C. *Inorg. Chim. Acta* **1995,** *235*, 51.

(18) Osborn, R. S.; Rogers, D. *J. Chem. Soc., Dalton Trans.* **1974**, 1002−1004.

(19) Hazell, A.; Simonsen, O.; Wernberg, O. *Acta Crystallogr.* **1986**, *C42*, 1707; Dong, V,; Endres, H.; Keller, H. J.; Morani, W.; Nöthe, D. *Acta Crystallogr.* **1977**, *C33*, 2428.

(20) (a) Collison, D.; Mabbs, F. E.; McInnes, E. J. L.; Taylor, K. J.; Welch, A. J.; Yellowlees, L. J. *J. Chem. Soc., Dalton Trans.* **1996**, 329. (b) McInnes, E. J. L.; Welch, A. J.; Yellowlees, L. J. *J. Chem. Soc., Chem. Commun.* **1996**, 2393−2394.

(21) Crozier, E. D.; Rehr, J. J.; Stern, E. A. In *X-ray Absorption: Principles, Applications and Techniques of EXAFS, SEXAFS and XANES*; Koninsberger, D. C., Prins, R., Eds.; John Wiley and Sons: New York, 1988; pp 373−432.

(22) Under the conditions used here, values of ^3J for free bpy were found to be (H6,6′) 4.78 Hz and (H3,3′) 7.98 Hz, while for $[Pt(bpy)_2][BF_4]_2$ they were found to be (H6,6′) 5.24 Hz and (H3, 3′) 8.14 Hz.

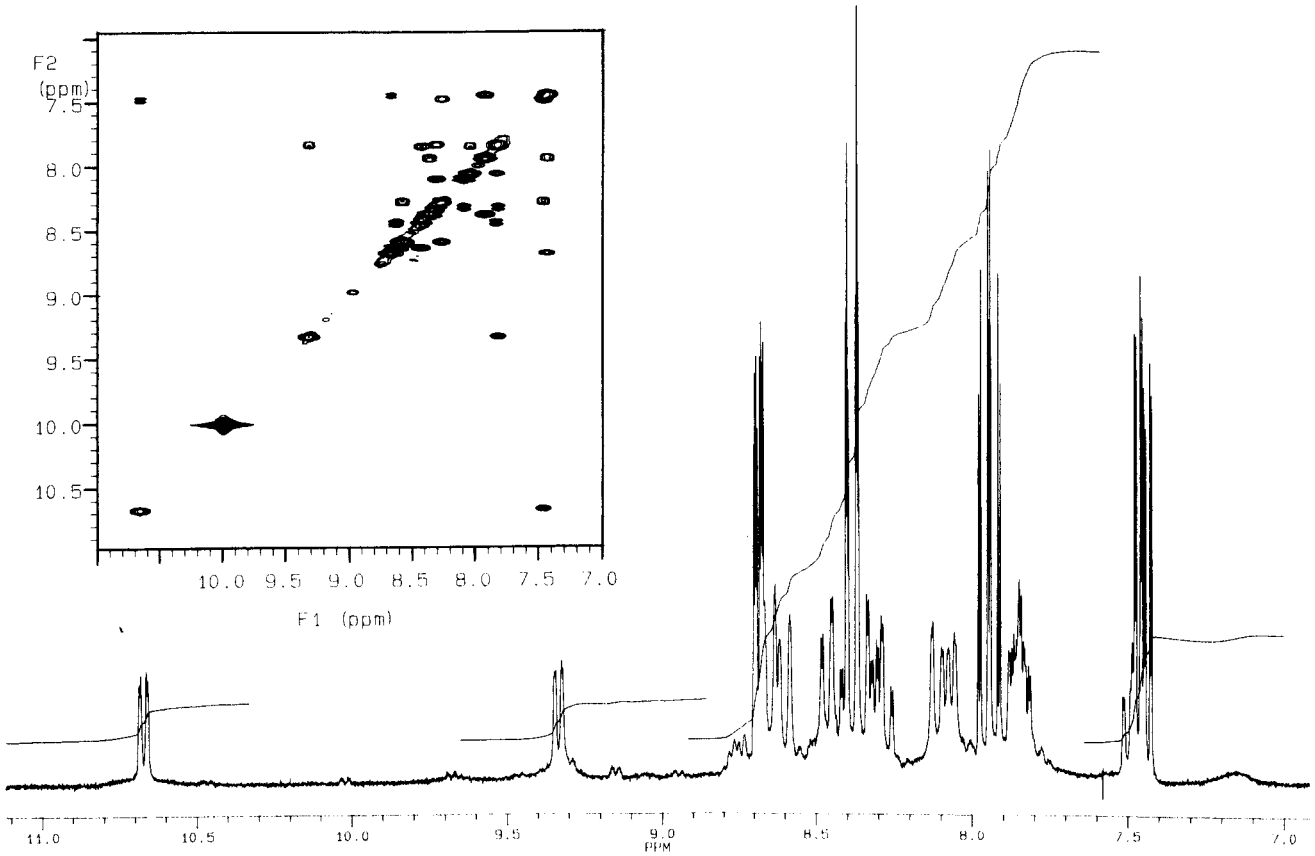

Figure 4. 1- and 2-D COSY ^{1}H NMR spectra of the reaction liquor after one electron reduction of $[Pt(bpy)_2][BF_4]_2$ in methyl sulfoxide-d_6.

Table 5. Summary of NMR Data for the Reaction Liquor after One-Electron Reduction of $[Pt(bpy)_2][BF_4]_2$ in Methyl Sulfoxide-d_6[a]

signal	chemical shift	^3J (Hz)	assignment
1	10.66	5.59 (d)	H111
2	9.31	5.67 (d)	H22
3	8.67	4.57	2,2′-bipyridyl H6,6′
4	8.62	8.03 (d)	H51
5	8.58	8.17 (d)	H81
6	8.43	7.55 (t)	H41
7	8.37	7.72	2,2′-bipyridyl H3,3′
8	8.31	7.85 (t)	H42
9	8.27	7.85 (t)	H91
10	8.09	8.04 (d)	H52
11	8.05	5.2 (d)	H21
12	7.93	7.79	2,2′-bipyridyl H4,4′
13	7.83	7.02 (dt)	H31
14	7.82	7.02 (dt)	H32
15	7.46	7.17 (t)	H101
16	7.45	6.15	2,2′-bipyridyl H5,5′

[a] Key: d, doublet; t, triplet; dt, doublet of triplets.

Kinetic parameters were determined for wave **1** in *N*,*N*′-dimethylformamide by comparison of digital simulations with real cyclic voltammograms. The ratio of reverse peak height to forward peak height, i_{pr}/i_{pf}, and thus the rate of the following reaction, was found to be independent of the concentration of starting material between 0.36 and 10.49 mmol dm^{-3}. Furthermore, addition of 2,2′-bipyridyl was found to enhance the degree of reversibility of the wave. Two mechanisms may then be proposed. Both commence with the reduction of $[Pt(bpy)_2]^{2+}$ to yield $[Pt(bpy)_2]^+$, which participates in an equilibrium, yielding free bpy and $[Pt(bpy)]^+$, or a solvated analogue of this species. The two possible mechanisms then diverge from their shared first step. In the first the coordinatively unsaturated species $[Pt(bpy)]^+$ attacks the platinum(II) starting material to yield $[Pt_2(bpy)_3]^{3+}$, followed by a rapid heterogeneous electron transfer to yield the final platinum(I) dimer. In the second, $[Pt(bpy)_2]^+$ is the substrate for attack, yielding the final product directly. These two mechanisms were easily distinguished by simulation. The former implies a sharp increase in the peak dimensionless current function, Λ, for the forward sweep of a cyclic voltammogram with increasing scan rate. The function Λ is given by $FAC_0(DF\nu/RT)^{1/2}$ where A is the electrode area, ν is the potential scan rate, and all other variables and constants have their usual meanings. The mechanism in which the reacting species are both Pt(I) implies a gradual decline in the value of this function with increasing scan rate, and this was the situation which was found experimentally, as shown in Table 6. The following mechanism was then assumed and the various constants were varied to maximize the fit between simulation and experiment.

Table 6. Experimental and Calculated Dimensionless Forward Peak Current Functions for the Reduction of $[Pt(bpy)_2][BF_4]_2$ in *N*,*N*-Dimethylformamide as a Function of Scan Rate

scan rate (V s^{-1})	Λ(exptl)	Λ(simtd)	scan rate (V s^{-1})	Λ(exptl)	Λ(simtd)
0.1	0.5373	0.4890	2.6	0.4776	0.4619
0.5	0.5163	0.4778	5	0.4625	0.4573
1	0.4964	0.4711	10	0.4561	0.4558

$$2[Pt(bpy)_2]^{2+} + 2e^- \underset{}{\overset{k_0}{\rightleftharpoons}} 2[Pt(bpy)_2]^+$$

$$[Pt(bpy)_2]^+ \underset{k_{1r}}{\overset{k_{1f}}{\rightleftharpoons}} [Pt(bpy)]^+ + bpy$$

$$[Pt(bpy)]^+ + [Pt(bpy)_2]^+ \xrightarrow{k_2} [Pt_2(bpy)_3]^{2+}$$

$$2\,[Pt(bpy)_2]^{2+} + 2e^- \longrightarrow [Pt_2(bpy)_3]^{2+} + bpy$$

Table 7. Experimental and Calculated Forward Peak Potentials (E_{pf}), Forward Peak Currents (i_{pf}), Reverse Peak Potentials (E_{pr}), and Reverse Peak Currents (i_{pr}) for the Reduction of $[Pt(bpy)_2][BF_4]_2$ in *N*,*N*-Dimethylformamide as a Function of Scan Rate[a]

scan rate ($V\ s^{-1}$)	simulated		experimental	
	E_{pf} (V), i_{pf} (μA)	E_{pr}(V), i_{pr} (μA)	E_{pf} (V), i_{pf} (μA)	E_{pr} (V), i_{pr} (μA)
5	−1.161, −20.43	−1.081, 1.316	−1.169, −20.49	−1.089, 1.695
10	−1.161, −28.90	−1.091, 5.749	−1.164, −28.67	−1.094, 5.284
50	−1.171, −0.141	−1.096, 0.067	−1.169, −0.142	−1.098, 0.069
100	−1.171, −0.217	−1.091, 0.106	−1.168, −0.180	−1.096, 0.087
500	−1.182, −0.474	−1.078, 0.256	−1.184, −0.471	−1.079, 0.250
1000	−1.191, −0.697	−1.071, 0.368	−1.199, −0.743	−1.071, 0.508

[a] Note that between 10 and 50 V s^{-1} the electrode diameter changes from 500 to 25 μm.

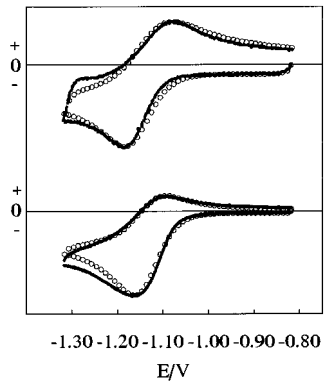

Figure 5. Demonstration of the closeness of fit for real (line) and calculated (open circles) voltammograms for the reduction of $[Pt(bpy)_2][BF_4]_2$ in *N*,*N*-dimethylformamide/0.2 mol dm^{-3} $[N^nBu_4][BF_4]$ at scan rates of 500 (upper data) and 10 (lower data) V s^{-1}. Note that the current scale is expanded 60 times for the upper data set.

Table 8. Experimental and Calculated Peak Current Ratios for the Reduction of $[Pt(bpy)_2][BF_4]_2$ (3 mmol dm^{-3}) in *N*,*N*-Dimethylformamide as a Function of the Concentration of Added 2,2′-Bipyridyl

concn of 2,2′-bipyridyl (mmol dm^{-3})	i_{pr}/i_{pf} (exptl)	i_{pr}/i_{pf} (simtd)	concn of 2,2′-bipyridyl (mmol dm^{-3})	i_{pr}/i_{pf} (exptl)	i_{pr}/i_{pf} (simtd)
0	0.183	0.184	300	0.210	0.251
30	0.184	0.189	1500	0.334	0.359
150	0.190	0.218	3000	0.437	0.414

Voltammograms recorded at high scan rate were used to determine, by simulation, the parameters for the heterogeneous electron transfer in the absence of the following chemical reactions. The optimum values were found to be $E_0 = -1.132$ V, $D = 2.2 \times 10^{-6}$ $cm^2\ s^{-1}$, $\alpha = 0.73$, and $k_0 = 0.15$ cm s^{-1}. These values were then used while the other parameters were varied for simulation of voltammograms at lower scan rates. The final values chosen to maximize the fit between simulation and experiment were $k_{1f} = 26\ s^{-1}$ and $k_2/k_{1r} = 770$. The values of k_2 and k_{1r} could not be determined independently, but the ratio was found to be the crucial variable in describing the response of the system to added bpy.

Two examples of real and simulated voltammograms at sweep rates of 10 and 500 V s^{-1} are shown in Figure 5, the peak currents and potentials being as given in Table 7. As can be seen, the fit is reasonable although not perfect as regards the width of the forward peaks. Peak height, separation, and ratio were taken as the characteristics to be optimized. Calculated and experimental values may be found in Table 7. The response of the system to added bpy is detailed in Table 8. The agreement obtained is reasonable considering that the physical properties of the medium were grossly altered by the presence of the free ligand at concentrations up to 3 mol dm^{-3}. Given the good agreement between voltammograms obtained and those calculated under a wide variety of conditions, the mechanism outlined above may be taken as substantially correct. All other waves for this system could be simulated assuming fast reversible electron transfers and the reactions initiated by the first electron transfer.

The cation $[Pt_2(bpy)_3]^{2+}$ is probably best regarded as the product of the insertion of a $[Pt(bpy)]^+$ fragment into the Pt−N bond of $[Pt(bpy)_2]^+$, which implies a weakening of this bond in the monomer, first for bpy loss, second as attack is preferred at the platinum (I) species rather than at platinum(II), which is itself quite electrophilic.[23] The mechanism determined, and particularly the fact that k_2 is 800 times greater than k_{1r}, the rate constant for re-attachment of bpy to $[Pt(bpy)]^+$, suggests that the interaction of the unpaired electron in $[Pt(bpy)_2]^+$ with the π^* orbitals of the ligand is weak, and only the formation of a weak Pt−Pt bond in the linear chain complex[7] allows the retention of the full ligand set. While a detailed discussion of the molecular orbital structure of the participating species is out of place here, and will be presented in a future paper, we note that the LUMO of the $[Pt(bpy)_2]^{2+}$ cation is unlikely to be primarily ligand-based as is the case[20] for most complexes of the form $[Pt^{II}(bpy)L_2]^{n+}$, which generally show electrochemically reversible first reductions.

Spectroscopic data would be required to assign waves **2** and **5** with any real certainty, which will prove difficult to obtain for such transient species. However, if one accepts the argument above, then these waves might be assigned to the first and second reductions of a bpy ligand. This is corroborated by the 600 mV separation between the waves typical of successive reductions of coordinated bpy ligands, the fast electron-transfer kinetics displayed, and the lack of any increase in the reactivity of the species generated compared to that generated in wave **1**. This in turn suggests that only one of the ligands is electroactive, and indeed the deviation from planarity[19] of one of the bpy ligands in $[Pt(bpy)_2]^{2+}$ is well documented, although they are equivalent by NMR in solution. Work is underway to make more definite assignments in this system.

Concluding Remarks

The complex electrochemical behavior of the $[Pt(bpy)_2]^{2+}$ cation in aprotic media has been resolved on the basis of the competition between three successive one-electron reductions of the starting material and a reaction initiated by the first of these three reductions. The product of this reaction is shown to be a platinum(I) dimer, $[Pt_2(bpy)_3]^{2+}$, containing a highly novel structural motif, a platinum−platinum bond supported by a bridging 2,2′-bipyridyl ligand. Its formation has been shown to proceed by an ECC mechanism where ligand loss from the reduced monomer is the rate-determining step in the concentra-

(23) (a) Farver, O.; Mønsted, O.; Nord, G. *J. Am. Chem. Soc.* **1979**, *101*, 6118−6119. (b) Livingstone, S. E.; Wheelahan, B. *Aust. J. Chem.* **1964**, *17*, 219.

tion range studied. In addition, bulk electrolysis without inert electrolyte has been used to isolate this dimeric product, something which had proved impossible in our laboratory by normal chemical and electrochemical techniques. We hope that the experimental procedure laid out in this paper will constitute a protocol for the study of transition metal complexes showing irreversible couples leading to reactive or unstable products, a potentially rich area of study often neglected. The principle of electrolysis without inert electrolyte can easily be extended to neutral complexes by the addition of exactly 1 equiv of electrolyte, the cations of which would then migrate through the frit during reduction, leaving the desired complex and, say, tetrafluoroborate as counterion.

Acknowledgment. We are very grateful to a number of people who willingly gave their time to help in this work, especially Dr. Ken Taylor, Dr. Scott Ingham, and Dr. Loïc Mottier. Professor Peter Sadler also has our thanks for access to the NMR spectrometer. The work was financed by a grant from the EPSRC.

Supporting Information Available: Design of cell employed for electrolysis without inert electrolyte, voltammograms recorded before and after electrolysis in this cell, tables of atomic coordinates and equivalent isotropic displacement parameters and anisotropic displacement parameters for $[Pt_2(bpy)_3][BF_4]_2$, and graphical evidence of the fit between theory and experiment for the model used in analysis of the EXAFS results (5 pages, print/PDF). See any current masthead page for ordering information and Web access instructions.

JA981670W